Available online at www.sciencedirect.com
SCIENCE DIRECT®
Journal of Solid State Chemistry 178 (2005) 2701–2708
JOURNAL OF SOLID STATE CHEMISTRY
www.elsevier.com/locate/jssc

Preparation and characterization of *trans*-RhCl(CO)(TPPTS)$_2$-intercalated layered double hydroxides

Xian Zhang[a], Min Wei[a], Min Pu[a], Xianjun Li[b], Hua Chen[b], David G. Evans[a], Xue Duan[a,*]

[a]*Key Laboratory of Science and Technology of Controllable Chemical Reactions, Ministry of Education, Box 98, College of College, Beijing University of Chemical Technology, Beijing 100029, P.R. China*
[b]*Department of Chemistry, Sichuan University, Chengdu 610064, China*

Received 5 April 2005; received in revised form 27 May 2005; accepted 13 June 2005
Available online 25 July 2005

Abstract

trans-RhCl(CO)(TPPTS)$_2$ (TPPTS = *tris*(*m*-sulfonatophenyl)phosphine) has been intercalated into Zn–Al layered double hydroxides (LDHs) by the method of ion exchange. The structure, composition and thermal stability of the composite material have been characterized by powder X-ray diffraction, Fourier transform infrared and ^{31}P solid-state magic-angle spinning nuclear magnetic resonance spectroscopy, elemental analysis, thermogravimetry, and differential thermal analysis. The geometry of *trans*-RhCl(CO)(TPPTS)$_2$ was fully optimized using the PM3 semiempirical molecular orbital method, and a schematic model for the intercalated species has been proposed. The thermal stability of *trans*-RhCl(CO)(TPPTS)$_2$ is significantly enhanced by intercalation, which suggests that such materials may have prospective application as the basis of a supported catalyst system for the hydroformylation of higher olefins.

Keywords: Layered double hydroxide; Hydrotalcite; TPPTS; *trans*-RhCl(CO)(TPPTS)$_2$; Intercalation

1. Introduction

Hydroformylation of alkenes using transition metal catalysts is widely applied in the petrochemical industry for the production of aldehydes (ca. 7 million tons per year) [1]. In the past three decades, considerable research has been devoted to the development of recyclable catalysts for hydroformylation [2]. Two-phase catalysis using complexes of water-soluble phosphines such as tris(*m*-sodiumsulfonatophenyl)phosphine (TPPTS-Na$_3$) [3] has been widely studied and finds large-scale application in the Ruhrchemie/Rhône Poulenc process, but has limited efficacy in the case of higher alkenes because of their low solubility in the aqueous medium. Fluorous biphasic catalysis with suitably fluorinated ligands in perfluorinated solvents [4], supercritical CO_2 [5] and ionic liquids [6] are other avenues which have been explored. Many attempts have also been made to support hydroformylation catalysts by covalent attachment to polymeric organic, inorganic or hybrid supports [7] but there are problems with catalyst stability and selectivity as well as leaching of the catalytic material. An alternative approach is the use of supported aqueous-phase catalysis (SAPC) in which the catalyst is immobilized in a thin layer of water adhering to the pore walls of a high surface area hydrophilic support such as controlled pore silica glass suggested by Davis and Hanson [8–12]. A number of other supports have also been used in SAPC including mesoporous zeolites [13], silica [14–17], apatitic tricalcium phosphate [18] and hydrophilic permutite [19]. Although high rates of hydroformylation have been observed using SAPC, the regioselectivity is low [2] and surprisingly little data have been reported on the recyclability and stability of these systems [2,11].

*Corresponding author. Fax: +86 010 6442 5385.
E-mail address: duanx@mail.buct.edu.cn (X. Duan).

0022-4596/$ - see front matter © 2005 Elsevier Inc. All rights reserved.
doi:10.1016/j.jssc.2005.06.008

Layered double hydroxides (LDHs) are a class of synthetic anionic clays whose structure can be described as containing brucite ($Mg(OH)_2$)-like layers in which some of the divalent cations have been replaced by trivalent ions giving positively charged sheets [20–22]. This charge is balanced by intercalation of anions in the hydrated interlayer regions. LDHs can be represented by the general formula $[M^{II}_{1-x}M^{III}_{x}(OH)_2]^{x+}(A^{n-})_{x/n}\cdot yH_2O$. The identities of the di- and trivalent cations (M^{II} and M^{III}, respectively) and the interlayer anion (A^{n-}) together with the value of the stoichiometric coefficient (x) may be varied over a wide range, giving rise to a large class of isostructural materials. LDHs are now well established as excellent anion-exchange materials and their extensive intercalation chemistry means they have widespread applications as anion exchangers, adsorbents, and as additives to plastics. There have also been some reports of intercalation of transition metal complexes in LDHs giving materials with expanded interlayer spacing which have shown good catalytic activity. Examples include dioxomolybdenum(VI) complexes [23], cobalt(II) macrocylic complexes [24] and manganese(III) complexes of Schiff base ligands [25]. In other cases, catalytic activity is observed with no expansion of interlayer spacing, suggesting that the catalytically active anion is adsorbed on edge sites as in the case of WO_4^{2-} [26] or $PdCl_4^{2-}$ [27].

The interlayer galleries of LDHs in which the anions are intercalated are extensively hydrated. Although the properties of water can be expected to be modified by adsorption on a surface (as in SAPC) or confinement in the interlayer galleries of an LDH [28], quasi-elastic neutron scattering measurements [29–31] and molecular dynamics simulations [32] have demonstrated that the water molecules are not fixed in one location in LDHs but rather exhibit translational diffusion as well as reorientational motions and that the relative mobility increases with increasing M^{II}/M^{III} ratio in the layers, which is associated with decreasing anion content and charge density on the layers. Furthermore, far IR spectroscopy and molecular dynamics simulations have demonstrated the structural and dynamic similarity of the interlayer Cl^- ions in LDHs to those in bulk aqueous solutions [33]. These results suggest that intercalation of a water-soluble hydroformylation catalyst in the highly hydrated galleries of a suitably tailored LDH represents an alternative to SAPC. Jones et al. [34] have shown that interlayer water is more strongly bound than physisorbed water by some 12 kJ mol^{-1}, suggesting that reactions with LDH-intercalated catalysts could be operated at higher temperatures than for SAPC. Furthermore, confinement of the catalyst in the interlayer galleries may reduce leaching compared with SAPC and stabilize the complex against decomposition.

To our knowledge, there has only been attempt to immobilize a water-soluble phosphine transition metal complex on an LDH viz. reaction of *cis*-Pd(TPPTS-Na_3)$_2Cl_2$ and Mg–Al–Cl LDH with ($Mg^{2+}/Al^{3+} = 3$) afforded a material with unchanged layer spacing indicating that the palladium complex is immobilized on the edge of the crystallites [35]. In this paper we report the reaction of a hydroformylation catalyst *trans*-RhCl(CO)(TPPTS-Na_3)$_2$ with Zn–Al–NO_3 LDHs having different Zn^{2+}/Al^{3+} ratios. The LDH precursors contained nitrate as interlayer anion because it is more readily replaced than chloride [36].

2. Experimental

2.1. Synthesis

TPPTS-Na_3 was prepared by the literature method [37]. *Trans*-RhCl(CO)(TPPTS-Na_3)$_2$ was synthesized according to the procedure described in a Chinese patent [38]. A solution of $RhCl_3\cdot 3H_2O$ (0.5 g, 1.90 mmol) in pure ethanol (10 mL) was held at 78 °C under carbon monoxide atmosphere for 50 min. Then heat was stopped and a solution of TPPTS-Na_3 (2.5 g, 5.0 mmol) in distilled, deionized water (5 mL) was added dropwise quickly. The mixture was held at 78 °C for 40 min. Pure ethanol was added to cold the mixture. The precipitate was separated, washed with pure ethanol and dried in vacuo at 80 °C for 4 h. Analysis: found (calculated) wt%: P 4.67, S 15.04, Rh 7.58, Na 16.02; P/Rh 1.9(2.0), S/P 2.9(3.0), Na/S 1.1(1.0), Na/P 3.1 (3.0).

The precursor $[Zn_2Al(OH)_6](NO_3)\cdot 4H_2O$, (represented as NO_3-Zn_2Al-LDH) was synthesized by a procedure similar to that described previously [39]. A solution of NaOH (11.2 g, 0.266 mol) in distilled, deionized water (100 mL) was added dropwise over 2 h to a solution of $Zn(NO_3)_2\cdot 6H_2O$ (35.6 g, 0.12 mol), $Al(NO_3)_3\cdot 9H_2O$ (22.6 g, 0.06 mol) and $NaNO_3$ (9.06 g, 0.106 mol) in distilled, deionized water (160 mL). The mixture was held at 70 °C under a nitrogen atmosphere for 24 h. The precipitate was separated by centrifugation, washed with water and dried at 70 °C for 18 h. Analysis: found (calculated) wt%: Zn 37.80, Al 8.45, Zn/Al 1.86. Other precursors $[Zn_3Al(OH)_8](NO_3)\cdot 4H_2O$ (represented as NO_3-Zn_3Al-LDH) and $[Zn_4Al(OH)_{10}](NO_3)\cdot 4H_2O$ (represented as NO_3-Zn_4Al-LDH) were synthesized in the same way with different Zn/Al molar ratios. Analysis: found (calculated) wt%: NO_3-Zn_3Al-LDH: Zn 44.17, Al 7.56, Zn/Al 2.43; NO_3-Zn_4Al-LDH: Zn 46.68, Al 5.32, Zn/Al 3.65.

Intercalation of the rhodium complex into LDHs was carried out by the method of ion exchange. A solution of *trans*-RhCl(CO)(TPPTS-Na_3)$_2$ (0.52 g, 0.45 mmol) in distilled, deionized water (10 mL) was added to a suspension of NO_3-Zn_2Al-LDH (0.64 g, 0.9 mmol) in water (40 mL) and the mixture was heated at 40 °C

under a nitrogen atmosphere for 24 h. The product was washed extensively with water, centrifuged and dried in vacuo at 50 °C. Other intercalates with different Zn/Al molar ratios were obtained by the same method.

2.2. Characterization

Powder X-ray diffraction (XRD) measurements were performed on a Rigaku XRD-6000 diffractometer, using Cu$K\alpha$ radiation ($\lambda = 0.154$ nm) at 40 kV, 30 mA, a scanning rate of 0.02°/s, and in the 2θ range 3–70°.

Fourier transform infrared (FT-IR) spectra were recorded using a Bruker Vector22 spectrophotometer in the range 4000–400 cm^{-1} with 2 cm^{-1} resolution. The standard KBr disk method (1 mg of sample in 100 mg of KBr) was used.

$^{31}P\{^{1}H\}$ nuclear magnetic resonance (NMR) solution spectra were recorded on a Bruker AV600 spectrometer operating at a frequency of 242.94 MHz for ^{31}P in D_2O solution with 85% H_3PO_4 as external reference. ^{31}P solid-state magic-angle spinning (MAS) NMR spectra was run on a Brucker AV300 spectrometer operating at a frequency of 121.497 MHz for ^{31}P at a spinning rate of ~5000 Hz with a 10 s pulse delay and referenced with respect to 85% H_3PO_4.

Elemental analysis was performed by inductively coupled plasma (ICP) emission spectroscopy on a Shimadzu ICPS-7500 instrument using solutions prepared by dissolving the samples in dilute HCl.

Thermogravimetric analysis and differential thermal analysis (TG–DTA) were measured in air using a PCT-1A thermal analysis system with a heating rate of 10 °C/min.

Semiempirical molecular orbital calculations were carried out on a Pentium VI computer using the PM3 method.

3. Results and discussions

Both the maximum content of a guest anion and the maximum amount of intrinsic water [40] that can be structurally accommodated in the galleries of an LDH will depend on the M^{II}/M^{III} ratio in the layers. In this work a series of LDHs with interlayer nitrate ions and different Zn/Al ratios were prepared and their intercalation reactions with *trans*-RhCl(CO)(TPPTS-Na_3)$_2$ were studied.

3.1. Structure of trans-RhCl(CO)(TPPTS)$_2$/LDH intercalates

The powder XRD patterns of the precursor NO_3-Zn_2Al-LDH and the materials produced by reaction of *trans*-RhCl(CO)(TPPTS-Na_3)$_2$ with LDHs having different Zn/Al molar ratios are shown in Fig. 1. The NO_3-Zn_2Al-LDH precursor has an XRD pattern similar to those reported previously [41], with a basal spacing (d_{003}) of 0.89 nm (Fig. 1a). After reaction with *trans*-RhCl(CO)(TPPTS-Na_3)$_2$, the powder XRD pattern of the product maintains the characteristic features of LDHs. The main diffraction peaks of *trans*-RhCl(CO)(TPPTS)$_2$-Zn_2Al-LDH structure appear at 5.07°(003), 9.84°(006), 19.32°(009), 60.95°(110), respectively, with an expanded basal spacing (d_{003}) of 1.74 nm (Fig. 1b). The peak at 19.32° 2θ might be the (006) reflection of little unchanged LDH-NO_3^- precursor, and the peak at 9.84° 2θ is the superposition of (003) reflection of the precursor and (006) reflection of the intercalation product. This indicates that there is very little of the unexchanged LDH-nitrate phase remaining in the product. The materials formed by reaction of *trans*-RhCl(CO)(TPPTS)$_2$ with LDHs having Zn/Al molar ratios of 3 and 4 have similar XRD patterns (Figs. 1c and 1d), with basal spacings (d_{003}) of 1.74 and 1.78 nm, respectively, indicating that the Zn/Al molar ratio has no remarkable influence on the intercalation of the guest. However, two peaks at around 11.56° 2θ and 23.55° 2θ were observed in Fig. 1c, which is possibly related to the presence of an LDH-CO_3^{2-} impurity phase that is often observed even when intercalation reactions are carried out under nitrogen. The two peaks can be assigned to the (003) and (006) reflections of LDH-CO_3^{2-} phase, respectively. The value of the basal spacing depends on the orientation of the interlayer anion and the water content as well as the average charge of the metal cations and there is relatively little difference between the values for the three *trans*-RhCl(CO)(TPPTS)$_2$-intercalated materials.

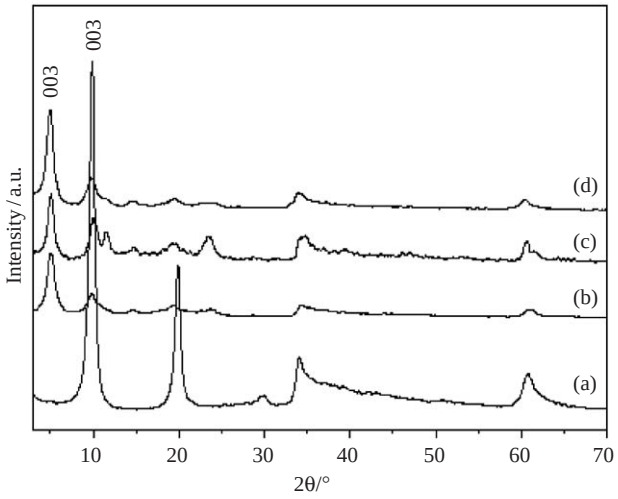

Fig. 1. Powder XRD patterns of (a) NO_3-Zn_2Al-LDH, (b) *trans*-RhCl(CO)(TPPTS)$_2$-Zn_2Al-LDH, (c) *trans*-RhCl(CO)(TPPTS)$_2$-Zn_3Al-LDH and (d) *trans*-RhCl(CO)(TPPTS)$_2$-Zn_4Al-LDH.

As noted above, reaction of *cis*-Pd(TPPTS)$_2$Cl$_2$ with an Mg-Al-Cl LDH with ($Mg^{2+}/Al^{3+} = 3$) failed to give

an intercalated palladium complex [35], whereas the *trans*-RhCl(CO)(TPPTS)$_2$ is readily intercalated. It may be that the *cis*-disposition of the TPPTS ligands in the former complex favors its immobilization on the edge of the crystallites, whereas a *trans*-disposition is more favorable to intercalation. It should also be noted however, that we chose an LDH-NO_3^- precursor rather than the Cl^- analog used in the case of the palladium complex.

3.2. IR spectroscopy of trans-RhCl(CO)(TPPTS)$_2$/LDH intercalates

Table 1 lists the main absorption bands in FT-IR spectra of *trans*-RhCl(CO)(TPPTS-Na$_3$)$_2$ and its intercalate in the LDH. The spectrum of *trans*-RhCl(CO)(TPPTS-Na$_3$)$_2$ is similar to that reported in the literature [42]. The bands at 1196, 1040 and 628 cm^{-1} can be attributed to the stretching vibrations of ν_{oso}, ν_{so} and ν'_{so}, respectively. After intercalation into the LDH host, all the three bands move to low frequency, at 1184, 1036 and 615–617 cm^{-1}, respectively. It is known that the coordination of the oxygen atom in the sulfonate group decreases the force constant in the S–O bond and thus also decreases the force constant in the vibration along this bond and accordingly shifts the location of the S–O vibration band to lower frequency [43], which has been reported in the FT-IR spectra of the intercalation of naphthalene-2,6-disulfonate [44,45] and 9,10-anthraquinone-1,2-dihydroxy-3-sulfonate (Alizarin red S anion) [46]. Therefore, it can be concluded that the shift of these bands in this work results from the interaction between the oxygen atom in the sulfonate group of the interlayer *trans*-RhCl(CO)(TPPTS)$_2$ and the host lattice. The ν_{CO} stretching vibration of the intercalated compounds are some 20 cm^{-1} higher than those of *trans*-RhCl(CO)(TPPTS-Na$_3$)$_2$ itself. All the other absorption bands of the *trans*-RhCl(CO)(TPPTS)$_2$-intercalated LDH, such as O–H stretching vibrations of both surface and interlayer water of LDH, phenyl ring vibrations and C–H out-of-plane bending vibrations of phenyl rings, are similar to those of the pristine *trans*-RhCl(CO)(TPPTS-Na$_3$)$_2$ [42]. All of the above data show that the *trans*-RhCl(CO)(TPPTS)$_2$ has been existed in the products without decomposition.

3.3. $^{31}P\{^1H\}$ NMR spectroscopy of trans-RhCl(CO)(TPPTS)$_2$/LDH intercalates

Figs. 2a and b show the $^{31}P\{^1H\}$ NMR spectra for TPPTS-Na$_3$ and *trans*-RhCl(CO)(TPPTS-Na$_3$)$_2$ in D_2O, respectively. For TPPTS-Na$_3$, the spectrum shows a single resonance at −5.7 ppm (Fig. 2a). This compares well to the literature value of −5.2 ppm [47]. For *trans*-RhCl(CO)(TPPTS-Na$_3$)$_2$ (Fig. 2b), a doublet is observed at 31.4 ppm (d; ^{1}J(Rh,P) 128 Hz), which is in agreement with the literature (31.3 ppm (d; ^{1}J(Rh,P) 128 Hz)) [48]. The ^{31}P MAS NMR spectrum obtained for *trans*-RhCl(CO)(TPPTS)$_2$ intercalated in the Zn$_2$Al-LDH (Fig. 2c) is consistent with the presence of *trans*-RhCl(CO)(TPPTS)$_2$ intercalated in the interlayer galleries of the LDH. No resonance due to the presence of free phosphine was observed at about −5 ppm. This indicates that *trans*-RhCl(CO)(TPPTS)$_2$ has been intercalated into LDH without decomposition, which is consistent with the results from IR spectroscopy and the value of d_{003} from XRD.

3.4. Chemical composition of trans-RhCl(CO)(TPPTS)$_2$/LDH intercalates

The molar elemental ratios of elements and chemical compositions of the *trans*-RhCl(CO)(TPPTS)$_2$/LDH intercalates are listed in Table 2. It should be noted that the water content of the three intercalates was calculated according to the weight loss below 150 °C on TG curves. The molar ratios P/Rh and S/P of the three materials are close to the theoretical values. There are some NO_3^- ions present in each of the materials,

Table 1
IR data for *trans*-RhCl (CO) (TPPTS-Na$_3$)$_2$ and *trans*-RhCl (CO) (TPPTS)$_2$/LDH

Type of vibration	*trans*-RhCl (CO) (TPPTS-Na$_3$)$_2$	*trans*-RhCl (CO) (TPPTS)$_2$-Zn$_2$Al-LDH	*trans*-RhCl (CO) (TPPTS)$_2$-Zn$_3$Al-LDH	*trans*-RhCl (CO) (TPPTS)$_2$-Zn$_4$Al-LDH
υ_{CO} (cm^{-1})	1973 (s)	1990 (m)	1990 (m)	1994 (m)
υ_{OSO} (cm^{-1})	1196 (vs)	1184 (vs)	1184 (vs)	1184 (vs)
υ_{SO} (cm^{-1})	1040 (vs)	1036 (vs)	1036 (vs)	1036 (vs)
υ'_{SO} (cm^{-1})	628 (s)	615 (m)	617 (m)	617 (m)
υ_{O-H} (cm^{-1})	3447 (s)	3447 (s)	3452 (s)	3445 (s)
	1636 (s)	1637 (s)	1637 (s)	1636 (s)
ν_{phenyl} (cm^{-1})	1466 (w)	1466 (s)	1466 (w)	1466 (w)
	1398 (m)	1400 (w)	1398 (m)	1398 (m)
γ_{C-H} (cm^{-1})	798 (s)	797 (m)	796 (m)	795 (m)
	690 (s)	685 (m)	690 (m)	690 (m)

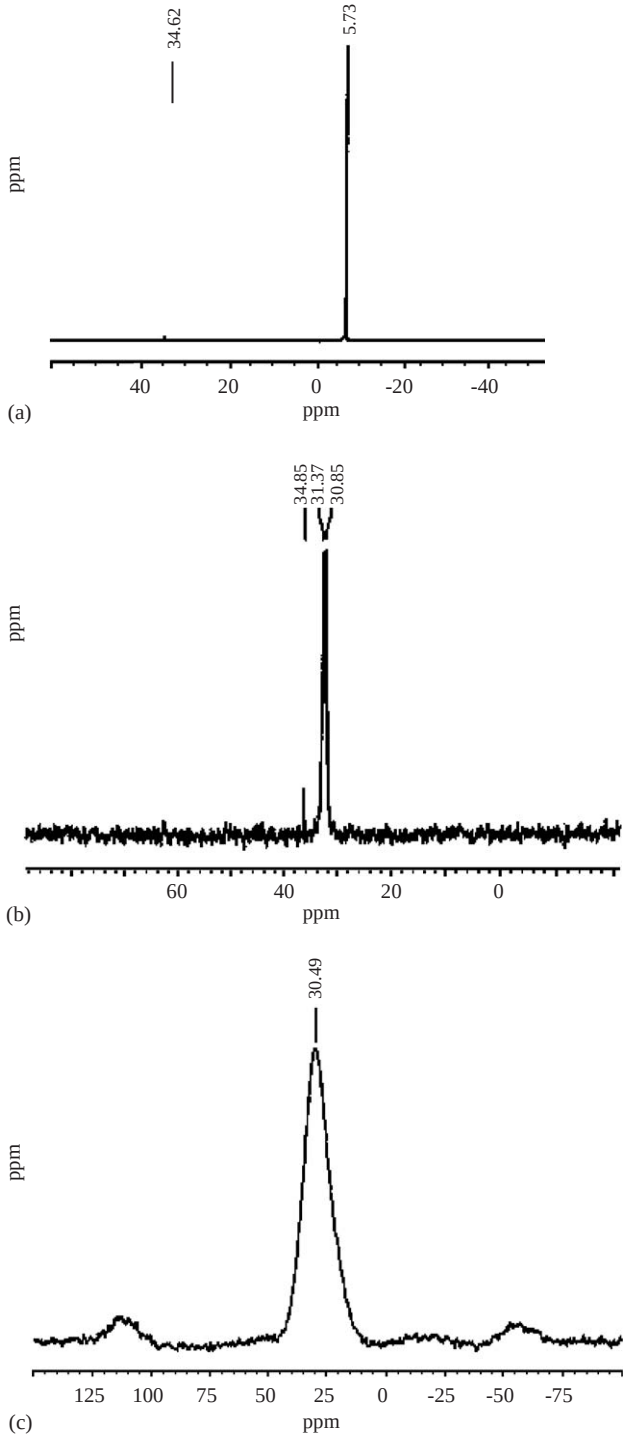

Fig. 2. $^{31}P\{^{1}H\}$ NMR spectra of (a) TPPTS in D_2O, and (b) *trans*-RhCl(CO)(TPPTS-Na_3)$_2$ in D_2O and (c) ^{31}P MAS NMR spectrum of *trans*-RhCl(CO)(TPPTS)$_2$-Zn_2Al-LDH.

indicating that exchange is incomplete. This is often observed when LDH-nitrate precursors are exchanged with larger anions [49].

As the Zn/Al molar ratio increases, the charge density of the brucite-like layers decreases, and as a result the content of intercalated *trans*-RhCl(CO)(TPPTS)$_2$ also decreases. In other words, the content of the guest can be controlled by changing the Zn/Al molar ratio of the host matrix. Table 2 confirms that the rhodium content of the materials decreases with increasing Zn/Al molar ratio as expected.

3.5. Structural model of *trans*-RhCl(CO)(TPPTS)$_2$/LDH intercalates

Since the interlayer distance in the *trans*-RhCl(CO)(TPPTS)$_2$/LDH intercalate Zn/Al = 2) is 1.74 nm and the thickness of the brucite layers is ca. 0.48 nm [50], the gallery height is 1.26 nm. An initial molecular model of RhCl(CO)(TPPTS)$_2$ was constructed using molecular mechanics methods. The geometry was then fully optimized by means of energy minimization and analytical gradient technology using the semiempirical PM3 molecular orbital method. The termination condition for rms gradient was 0.1 kcal/(A mol). According to the calculations, the maximum dimension of the anion is 1.24 nm. Comparison with the gallery height of 1.26 nm suggests that the *trans*-RhCl(CO)(TPPTS)$_2$ anions are accommodated in the interlayer region as a monolayer with the sulfonate groups interacting with both upper and lower hydroxide layers as shown in Fig. 3.

3.6. TG and DTA analysis of *trans*-RhCl(CO)(TPPTS-Na_3)$_2$ and *trans*-RhCl(CO)(TPPTS)$_2$/LDH intercalates

The TG curves for pristine *trans*-RhCl(CO)(TPPTS-Na_3)$_2$ and *trans*-RhCl(CO)(TPPTS)$_2$/LDH intercalates are shown in Fig. 4, and Fig. 5 displays the corresponding DTA curves. In the case of *trans*-RhCl(CO)(TPPTS-Na_3)$_2$ (Fig. 4a), three weight loss events are observed. The first event (30–120 °C) is attributed to the loss of adsorbed water, the second event (120–360 °C) is due to the decomposition of *trans*-RhCl(CO)(TPPTS-Na_3)$_2$ whilst the third sharp weight loss (360–440 °C) is the result of further decomposition as well as combustion of the material, with a corresponding strong exothermic peak in the DTA curve around 400 °C (Fig. 5a). The thermal decomposition of the *trans*-RhCl(CO)(TPPTS)$_2$-Zn_2Al-LDH is characterized by four steps (Fig. 4b). The weight loss event corresponds to the dehydration of water molecules physisorbed at the external surfaces of the crystallites and that of interlayer water molecules more strongly attached by hydrogen bonding overlap somewhat, in the temperature range 30–150 °C. The second event (150–293 °C) is due to the decomposition of the interlayer anions. The third (293–470 °C) is a consequence of dehydroxylation of the brucite-like layers and continued decomposition of interlayer anions. The fourth stage (470–528 °C) can be attributed to decomposition and combustion of

Table 2
Elemental analytical data for *trans*-RhCl (CO) (TPPTS-Na_3)$_2$ and *trans*-RhCl (CO) (TPPTS)$_2$/LDH

Sample	*trans*-RhCl (CO) (TPPTS-Na_3)$_2$	*trans*-RhCl (CO) (TPPTS)$_2$-Zn_2Al-LDH	*trans*-RhCl (CO) (TPPTS)$_2$-Zn_3Al-LDH	*trans*-RhCl (CO) (TPPTS)$_2$-Zn_4Al-LDH
P (w/w) (%)	4.67	1.71	1.70	1.29
S (w/w) (%)	15.04	5.35	5.40	4.19
Na (w/w) (%)	16.02	0	0	0.90
Rh (w/w) (%)	7.58	2.92	2.66	2.14
Zn (w/w) (%)	—	24.81	31.75	29.13
Al (w/w) (%)	—	5.64	5.80	3.20
Molar ratio of P/Rh	1.9	1.95	2.13	2.00
Molar ratio of S/P	2.9	3.03	3.08	3.15
Molar ratio of Na/S	1.1	0	0	0.30
Molar ratio of Zn/Al	—	1.83	2.28	3.79
Chemical composition		$[Zn_{0.647}Al_{0.353}(OH)_2]\{RhCl[CO][P(mC_6H_4SO_3)_3]_2\}_{0.0478}(NO_3)_{0.0671}\cdot 1.00H_2O$	$[Zn_{0.695}Al_{0.305}(OH)_2]\{RhCl[CO][P(mC_6H_4SO_3)_3]_2\}_{0.0367}(NO_3)_{0.0850}\cdot 0.82H_2O$	$[Zn_{0.791}Al_{0.209}(OH)_2]\{RhCl[CO][P(m\text{-}C_6H_4SO_3Na)(mC_6H_4SO_3)_2]_2\}_{0.0366}(NO_3)_{0.0626}\cdot 1.36H_2O$

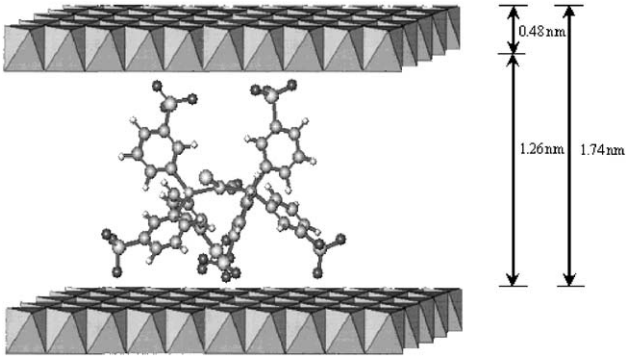

Fig. 3. A schematic representation of the possible arrangement in *trans*-RhCl(CO)(TPPTS)$_2$/LDH.

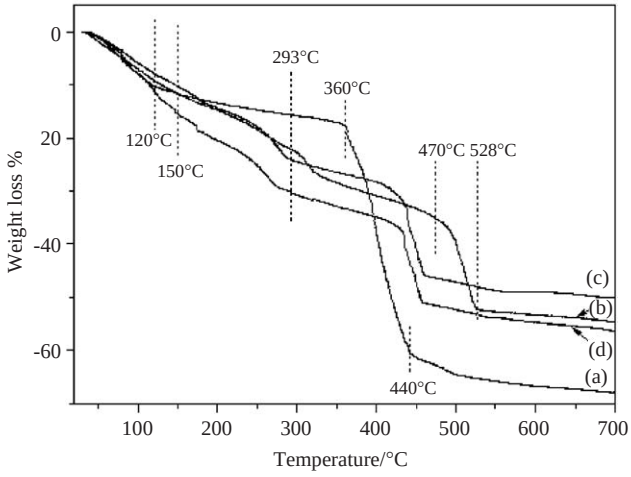

Fig. 4. TG curves of (a) *trans*-RhCl(CO)(TPPTS-Na_3)$_2$, (b) *trans*-RhCl(CO)(TPPTS)$_2$-Zn_2Al-LDH, (c) *trans*-RhCl(CO)(TPPTS)$_2$-Zn_3Al-LDH and (d) *trans*-RhCl(CO)(TPPTS)$_2$-Zn_4Al-LDH.

intercalated complex anions. The corresponding strong exothermic peak is observed at 510 °C in the DTA curve (Fig. 5b). Compared with the decomposition process for pure *trans*-RhCl(CO)(TPPTS)$_2$ (Fig. 5a), the decomposition of the intercalated anion is postponed and the combustion temperature is increased by some 110 °C by intercalation. This significant increase in thermal stability may be a result of the host–guest interactions present after intercalation. This suggests that the composite material may have prospective application as a catalyst for hydroformylation of higher olefins at higher temperatures, at which the homogeneous catalyst would decompose.

The TG/DTA curves of *trans*-RhCl(CO)(TPPTS)$_2$/LDH intercalates with Zn/Al = 2.3 (Fig. 4c and Fig. 5c) and Zn/Al = 3.8 (Fig. 4d and Fig. 5d) are rather similar to those for the case of Zn/Al = 1.8 (Fig. 4b and Fig. 5b) except that the temperatures of the corresponding weight loss events are reduced. This might be related to the higher Zn/Al molar ratios resulting in lower content of intercalated guest, and consequently less hindrance of interlayer diffusion and easier decomposition of the guest.

4. Conclusions

Trans-RhCl(CO)(TPPTS)$_2$/LDH intercalates have been obtained by ion exchange of *trans*-RhCl(CO) (TPPTS-Na_3)$_2$ with zinc-aluminum-nitrate LDHs with different Zn/Al molar ratios. XRD confirms the formation of intercalated species, with basal spacings of 1.74–1.78 nm. The interactions between host and

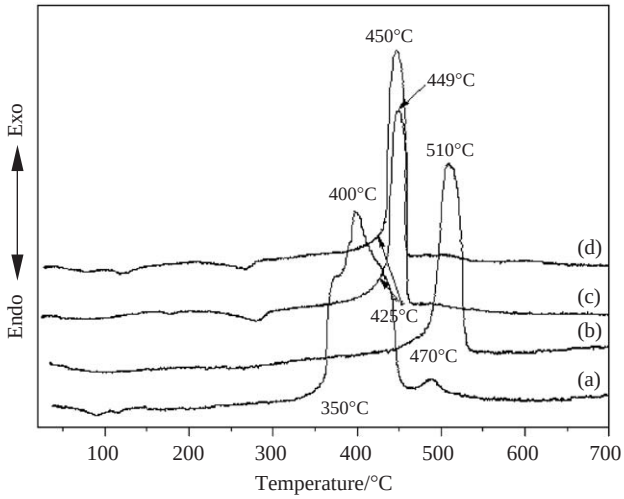

Fig. 5. DTA curves of (a) *trans*-RhCl(CO)(TPPTS-Na_3)$_2$, (b) *trans*-RhCl(CO)(TPPTS)$_2$-Zn_2Al-LDH, (c) *trans*-RhCl(CO)(TPPTS)$_2$-Zn_3Al-LDH and (d) *trans*-RhCl(CO)(TPPTS)$_2$-Zn_4Al-LDH.

guest were investigated by FT-IR and ^{31}P MAS NMR spectroscopy which indicate that *trans*-RhCl(CO)(TPPTS)$_2$ has been intercalated into LDH without decomposition. A structural model for the intercalates has been proposed based on the optimized geometry of *trans*-RhCl(CO)(TPPTS)$_2$. The anions are accommodated in the interlayer region as a monolayer with the sulfonate groups interacting simultaneously with both upper and lower hydroxide layers. It has been confirmed by elemental analysis that the content of the guest can be controlled by changing the Zn/Al molar ratio of the host matrix, which may have an influence on the catalytic activity of the composite material. The thermal stability of *trans*-RhCl(CO)(TPPTS)$_2$ is significantly enhanced by intercalation. Therefore, the intercalation of such rhodium complexes into LDHs may have potential applications in the development of novel supported aqueous-phase catalysts for hydroformylation of higher olefins.

Acknowledgments

This project was supported by the National Natural Science Foundation of China (Grant No. 90306012) and the Beijing Nova Program (No. 2004A13).

References

[1] G. Cum, P. Famulari, M. Marchetti, B. Sechi, J. Mol. Catal. A: Chem. 218 (2004) 211.
[2] P.W.N.M. van Leeuwen, A.J. Sandee, J.N.H. Reek, P.C.J. Kamer, J. Mol. Catal. A: Chem. 182-3 (2002) 107.
[3] E.G. Kuntz, O.M. Vittori, J. Mol. Catal. A: Chem. 129 (1998) 159.
[4] D.F. Foster, D. Gudmunsen, D.J. Adams, A.M. Stuart, E.G. Hope, D.J. Cole-Hamilton, G.P. Schwarz, P. Pogorzelec, Tetrahedron 58 (2002) 3901.
[5] M.F. Sellin, P.B. Webb, D.J. Cole-Hamilton, Chem. Commun. (2001) 781.
[6] P.B. Webb, M.F. Sellin, T.E. Kunene, S. Williamson, A.M.Z. Slawin, D.J. Cole-Hamilton, J. Am. Chem. Soc. 125 (2003) 15577.
[7] M. Lenarda, R. Ganzerla, L. Riatto, L. Storaro, J. Mol. Catal. A: Chem. 187 (2002) 129.
[8] J.P. Arhancet, M.E. Davis, J.S. Merola, Nature 339 (1989) 454.
[9] J.P. Arhancet, M.E. Davis, J.S. Merola, B.E. Hanson, J. Catal. 121 (1990) 327.
[10] J.P. Arhancet, M.E. Davis, B.E. Hanson, Catal. Lett. 11 (1991) 129.
[11] J.P. Arhancet, M.E. Davis, B.E. Hanson, J. Catal. 129 (1991) 94.
[12] J.P. Arhancet, M.E. Davis, B.E. Hanson, J. Catal. 129 (1991) 100.
[13] Y. Cai, Y.Z. Yuan, Q.J. Fu, Y.Q. Yang, Q.R. Cai, J. Xiamen Univ. (Nat. Sci.) 39 (2000) 128 (in Chinese).
[14] M. Benaissa, U.J. Jáuregui-Haza, I. Nikov, A.M. Wilhelm, H. Delmas, Catal. Today 79-80 (2003) 419.
[15] H.J. Zhu, Y.J. Ding, H.M. Yin, L. Yan, J.M. Xiong, Y. Lu, H.Y. Luo, L.W. Lin, Appl. Catal. A: Gen. 245 (2003) 111.
[16] Z.H. Li, Q.R. Peng, Y.Z. Yuan, Appl. Catal. A: Gen. 239 (2003) 79.
[17] Z.H. Li, W. Cao, Q.R. Peng, Y.Z. Yuan, J. Mol. Catal. (China) 15 (2001) 419 (in Chinese).
[18] M. Dessoudeix, U.J. Jáuregui-Haza, M. Heughebaert, A.M. Wilhelm, H. Delmas, A. Lebugle, P. Kalck, Adv. Synth. Catal. 344 (2002) 406.
[19] W.L. Cao, B. Tang, J.C. Zhang, B. Yan, J. Mol. Catal. (China) 15 (2001) 335 (in Chinese).
[20] F. Cavani, F. Trifero, A. Vaccari, Catal. Today 11 (1991) 173.
[21] A.I. Khan, D. O'Hare, J. Mater. Chem. 12 (2002) 3191.
[22] V. Rives (Ed.), Layered Double Hydroxides: Present and Future, Nova Science Publishers, New York, 2001.
[23] A. Corma, V. Fornes, F. Rey, A. Cervilla, E. Llopis, A. Ribera, J. Catal. 152 (1995) 237.
[24] T.J. Pinnavaia, M. Chibwe, V.R.L. Constantino, S.K. Yun, Appl. Clay Sci. 10 (1995) 117.
[25] S. Bhattacharjee, J.A. Anderson, Chem. Commun. (2004) 554.
[26] B. Sels, D. De Vos, M. Buntinx, F. Pierard, A. Kirsch-De Mesmaeker, P. Jacobs, Nature 400 (1999) 855.
[27] B.M. Choudary, S. Madhi, N.S. Chowdari, M.L. Kantam, B. Sreedhar, J. Am. Chem. Soc. 124 (2002) 14127.
[28] J. Wang, A.G. Kalinichev, R.J. Kirkpatrick, Geochim. Cosmochim. Acta 68 (2004) 3351.
[29] W. Kagunya, J. Phys. Chem. 100 (1996) 327.
[30] W. Kagunya, P.K. Dutta, Z. Lei, Physica B 234-6 (1997) 910.
[31] S. Mitra, A. Pramanik, D. Chakrabarty, R. Mukhopadhyay, Pramana—J. Phys. 63 (2004) 437.
[32] S.P. Newman, S.J. Williams, P.V. Coveney, W. Jones, J. Phys. Chem. B 102 (1998) 6710.
[33] J.W. Wang, A.G. Kalinchev, J.E. Amonette, R.J. Kirkpatrick, Am. Mineral. 88 (2003) 398.
[34] L. Pesic, S. Salipurovic, S. Markovic, D. Vucelic, W. Kagunya, W. Jones, J. Mater. Chem. 2 (1992) 1069.
[35] B.M. Choudary, M.L. Kantam, N.M. Reddy, N.M. Gupta, Catal. Lett. 82 (2002) 79.
[36] S. Miyata, Clays Clay Miner. 31 (1983) 305.
[37] E. Kuntz, US Patent 4,248,802, 1978.
[38] X.J. Li, H. Chen, Y.Z. Li, H.C. Liu, Chinese Patent CN1179429, 1998 (in Chinese)
[39] M.A. Drezdon, US Patent 4,774,212, 1988.
[40] S.K. Yun, T.J. Pinnavaia, Chem. Mater. 7 (1995) 348.
[41] Z.P. Xu, H.C. Zeng, J. Phys. Chem. B 105 (2001) 1743.

[42] W.A. Herrmann, J. Kellner, H. Riepl, J. Organomet. Chem. 389 (1990) 103.
[43] K. Nakanishi (Ed.), IR Absorption Spectroscopy—Practical, Nankodo, Tokyo, 1960.
[44] E. Kanezaki, Mater. Res. Bull. 34 (1999) 1435.
[45] E. Kanezaki, J. Incl. Phen. 36 (2000) 447.
[46] E. Kanezaki, J. Incl. Phen. Macrocyclic Chem. 46 (2003) 89.
[47] W.A. Herrmann, J.A. Kulpe, J. Kellner, H. Riepl, H. Bahrmann, W. Konkel, Angew Chem. Int. Ed. Engl. 29 (1990) 391.
[48] W.A. Herrmann, J.A. Kulpe, W. Konkol, H. Bahrmann, J. Organomet. Chem. 389 (1990) 85.
[49] N.T. Whilton, P.J. Vickers, S. Mann, J. Mater. Chem. 7 (1997) 1623.
[50] A. Cervilla, A. Corma, V. Fornes, E. Llopis, P. Palanca, F. Rey, A. Ribera, J. Am. Chem. Soc. 116 (1994) 1595.